

Simulated model studies for solid waste storage surveillance facility

Vishnu Verma *, A.K. Ghosh, H.S. Kushwaha

Reactor Safety Division, Bhabha Atomic Research Centre, Engg. Hall No. 7, Trombay, Mumbai 400 085, India

Received 28 May 2001; received in revised form 3 September 2001; accepted 17 September 2001

Abstract

High level radioactive waste generated from reprocessing of spent fuel from nuclear reactors are encased in canisters after vitrification. They have high heat generation rate and need interim storage under surveillance and are to be cooled continuously until major portion of the heat is dissipated. Natural circulation air cooling (using suitable stack dimensions) has been considered to cool the overpacks containing canisters. Thermal analysis has been carried out for a reduced scale model of such a facility. Theoretical and experimental results have been compared. © 2002 Elsevier Science B.V. All rights reserved.

1. Introduction

High level radioactive waste (HLW) is produced during reprocessing of spent fuel from a reactor. The radionuclides of HLW are immobilised in borosilicate glass matrix called as vitrified waste. High level radioactive waste has a high heat generation rate and cannot be transported immediately to the disposal site due to radiological hazard and high unit cost. The waste needs to be cooled adequately to avoid any failure of the matrix and leaching of the radioactive nuclei (Ozarde et al., 1981).

The radioactive waste material recovered after the vitrification process is encased in a cylindrical stainless steel canister. The canister is encased in

cylindrical overpack (also called as storage unit) (Fig. 1). A small annular air gap (R2–R3) is provided between the canister and the overpack for easy insertion of canisters into the overpack. Depending upon the design an overpack may contain one or more canisters. This ensures containment of radioactivity in the event of any accidental rupture of the canister containing the vitrified waste. The overpacks are placed in a storage vault. The product needs to be cooled continuously for structural integrity and to avoid leaching of the radioactive nuclides. From reliability consideration, it is advantageous to have a passive system of cooling. A stack has been provided to facilitate natural draught. A schematic of the system is shown in Fig. 2 and Fig. 3.

The present paper describes the cooling of the canisters of a typical solid waste storage surveillance facility (Verma et al., 1995a). It employs an

* Corresponding author. Tel.: +91-22-5593774; fax: +91-22-5505151.

E-mail address: vishnuv@magnum.barc.ernet.in (V. Verma).

axial flow arrangement in which the air flows axially over the storage unit. Air from the inlet duct is introduced at the bottom plenum of all the storage units. The flow emerging from the top of each storage unit is combined at the top plenum and goes to the stack. The air flow in the annular space between sleeve and overpack gets heated and rises due to buoyancy. The hot air in the stack rises through the stack due to buoyancy. The sleeve is used to guide the airflow.

Within the storage unit, the small annular air gap should be as small as possible from heat transfer point of view. There will be some natural circulation within the air gap. However, for a conservative estimate of canister centre line temperature only conduction within the gap has been considered.

Design limits are:

1. Centre line temperature of the canister should be kept below $500\text{ }^{\circ}\text{C}$ to avoid reformation of vitrified waste.
2. In the long run concrete temperature should be below $65\text{ }^{\circ}\text{C}$ to avoid dehydration of concrete.
3. There should be a minimum stack exit air velocity to avoid downwash due to the wind velocity. Minimum exit velocity depends upon the wind velocity.

A 1-D analysis has been carried out in which converged flow rate (by natural convection) has been obtained for various values of heat generation rate. Suitable stack dimensions and duct dimensions conforming to the design limits have been chosen based on a parametric study (Verma

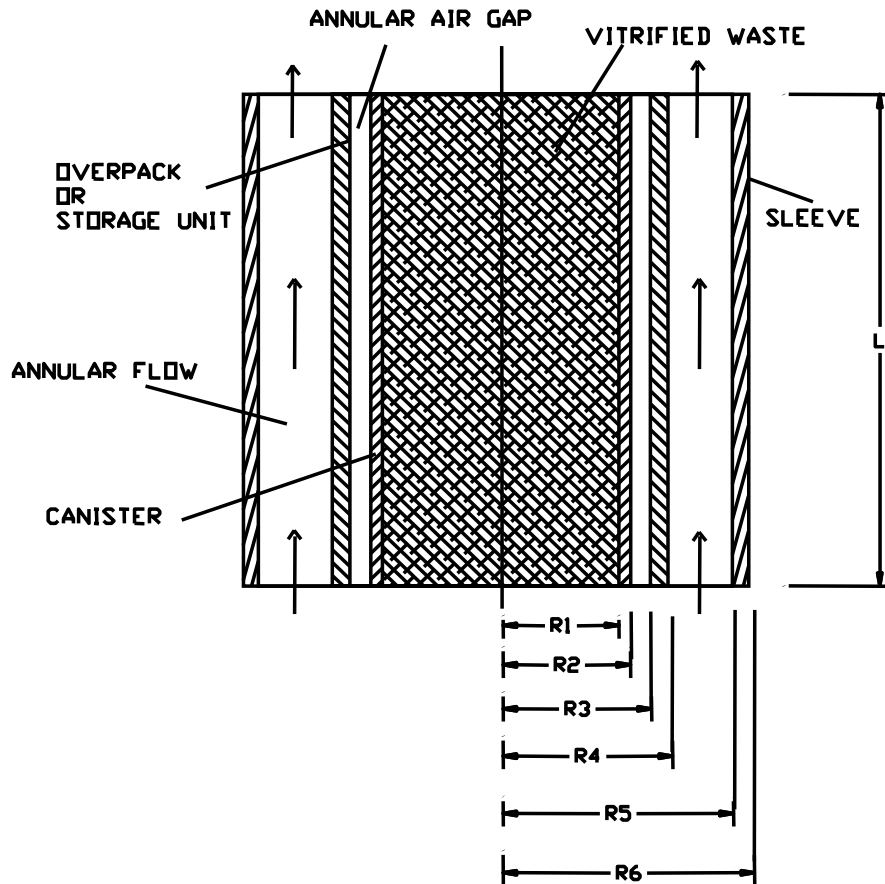


Fig. 1. Details of storage unit.

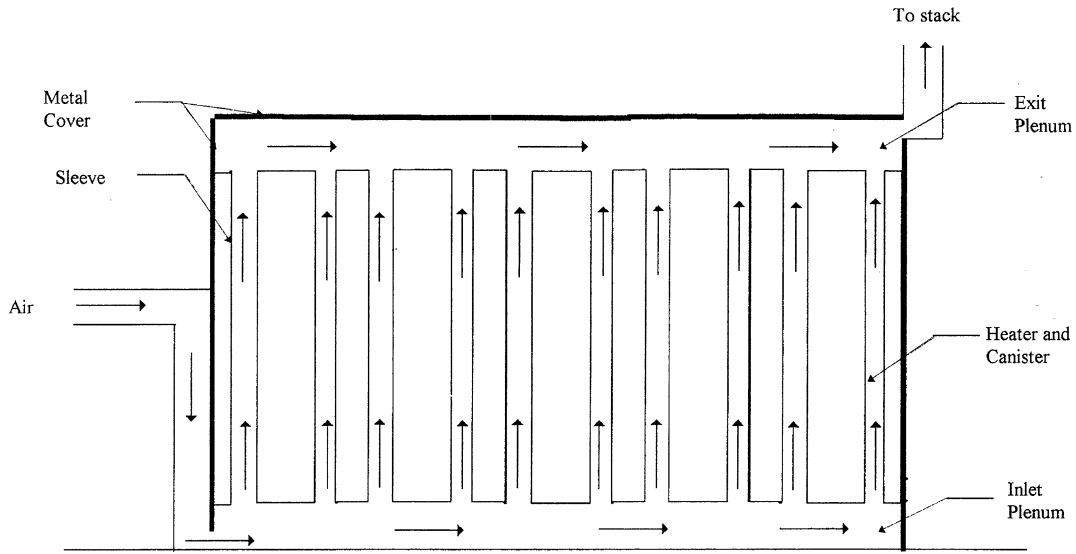


Fig. 2. Schematic view of the experimental setup.

et al., 1995a,b). The theoretical results obtained needed to be validated through experiments.

This paper describes the theoretical basis of the analysis, the experimental set up and compares the theoretical and the experimental results.

2. Theoretical analysis

The natural convection of air is primarily due to the heat generated in the canisters and subsequently transferred to the air flowing through the sleeve and further facilitated by the draft induced by the stack. The analysis is based on the solution of 1-D steady state equations of conservation of momentum and energy together with the continuity equation for flow of air by an iterative method.

Momentum Equation

$$V \frac{\partial V}{\partial Z} = -\frac{1}{\rho} \frac{\partial P}{\partial Z} - \frac{f_w V^2}{2D_e} - g \cos \theta, \quad (1)$$

Continuity Equation

$$\rho A V = \text{constant}, \quad (2)$$

Energy Equation

$$Q = hA \Delta T = \dot{m} C_p \Delta T_r, \quad (3)$$

Equation of state

$$\rho = \rho(P, T), \quad (4)$$

After integrating over the flow path, the steady state momentum equation (Eq. (1)) can be given for each section as:

$$P_i - P_{i+1} = \frac{4fL\rho V^2}{2D_e} + C_g \frac{\rho V^2}{2} + \bar{\rho} g L \cos \theta. \quad (5)$$

For the Fanning equation, the friction factor (f), is equivalent to 1/4th of the friction factor (f_w), (Darcy–Weisbach equation).

Where V is the velocity, Z is the axial distance, f is the fanning friction factor, $\bar{\rho}$ is the average density, and C_g is loss coefficient, which depends upon the geometry. The maximum value of C_g for abrupt expansion is equal to 1.0 and 0.5 for abrupt contraction. θ is the angle from the vertical.

The four equations (Eqs. (2)–(5)) are solved to obtain the four variables (V , ρ , T , P). Transfer parameter are related to the main variables mentioned above; for example:

$$f \text{ (friction factor)} = f(V) \quad (6)$$

which can be evaluated as (Kundsen et al., 1958)

$f = 0.079 Re^{-0.25}$ for turbulent flow,

$Re < 10^6$ (Blasius equation),

$f = 16/Re$ for laminar flow.

The buoyancy force generated due to density difference between the inside hot air and outside cold air will stabilise the flow such that it will overcome all the losses in the vault, duct and the stack.

Hence for all the sections Eq. (5) can be modified as:

$$g(Z_{\text{vault}} + Z_{\text{stack}})\rho_{\infty} = \sum_{i=1}^N (P_i - P_{i+1}), \quad (7)$$

where N is the number of sections, ρ_{∞} is the density of the outside air.

The scheme of the numerical computation is shown in Fig. 4.

Heat balance equation for the storage unit is given as:

$$Q = \pi R_1^2 q' L = Q_r + Q_c, \quad (8)$$

where q' is the heat generation rate per unit volume and L is the height of the canister, Q_r and

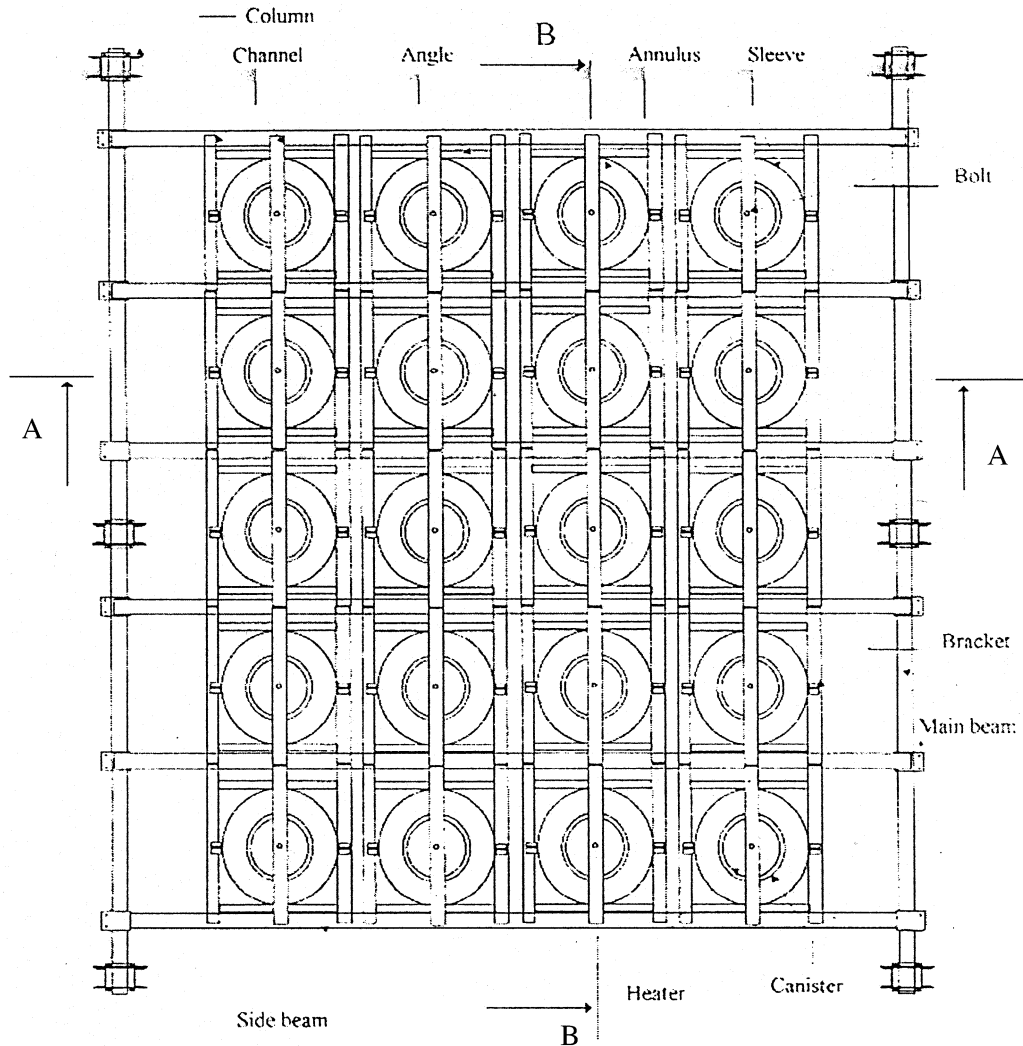


Fig. 3. Top view of the storage unit (overpack) and its support.

FLOW DIAGRAM

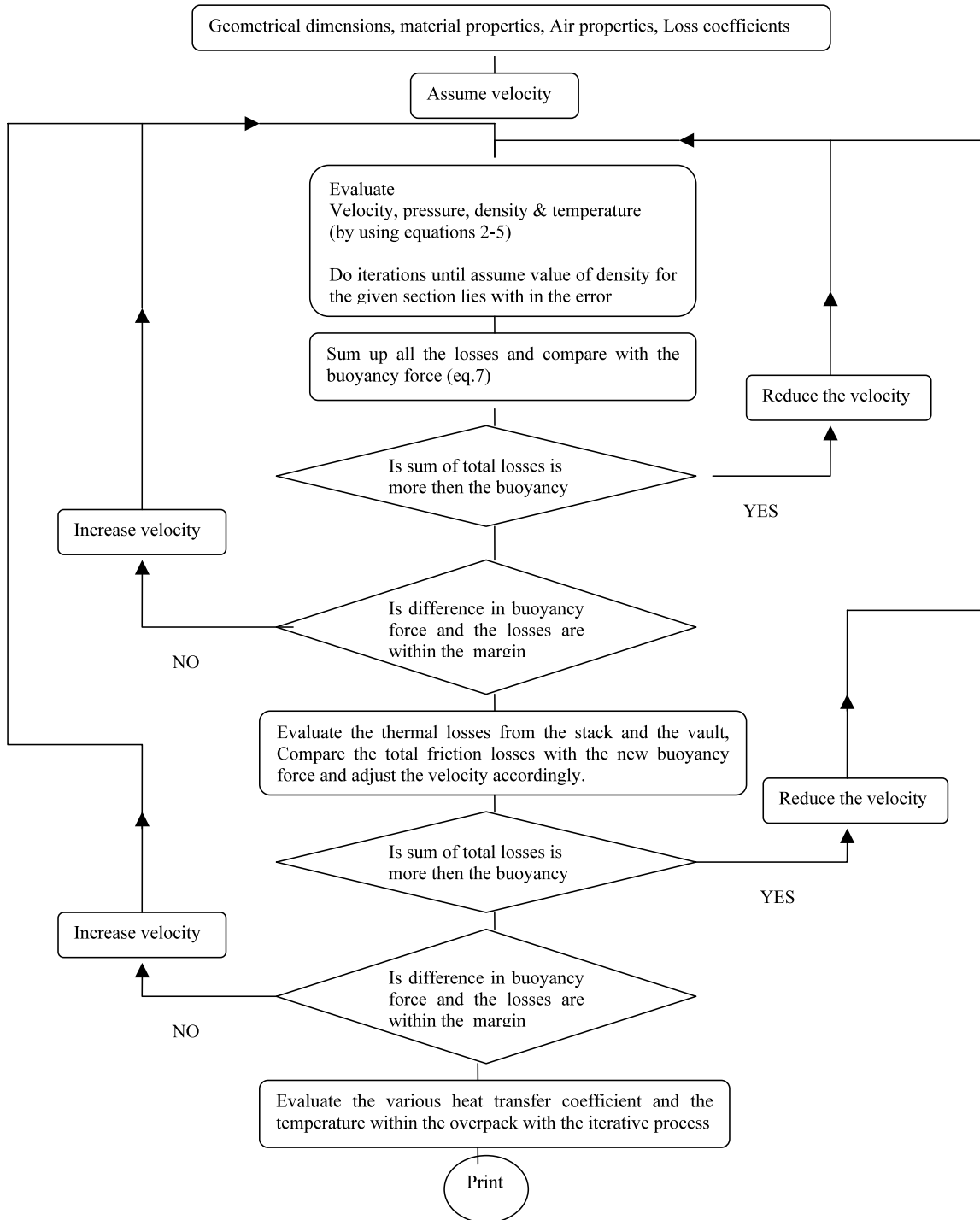


Fig. 4. Flow chart of the numerical analysis.

Table 1
Details of instrumentation

	Location							
	Overpack surface temperature	Sleeve surface temperature	Inlet of the annulus	Outlet of the annulus	Upper plenum	Stack inlet	Stack outlet	Reference
No. of thermocouple	12 ^a	12 ^a	3 ^b	3 ^b	2 ^c	1	1	4

Total number of thermocouples per overpack = 32. DAS (Data Acquisition System): channel capacity = 80. Two overpacks can be scanned at a time.

^a At four different elevation 0.5, 1.05, 1.5, and 1.95 m from the lower end of the overpack. Three thermocouple in each plane 120° apart.

^b One hundred and twenty degree apart.

^c One at the centre and other close to the roof of the upper plenum.

Q_c are the rates of heat transfer by radiation and convection respectively,

$$Q_r = \sigma \varepsilon (T_{su}^4 - T_{sl}^4) A_{su}, \quad (9)$$

$$= h_r A_{su} (T_{su} - T_{sl}), \quad (10)$$

where ε is the equivalent emissivity considering the storage unit and the sleeve surface, which can be given as (Wong, 1977)

$$\varepsilon = \left[\frac{1}{\varepsilon_{su}} + \frac{A_{su}}{A_{sl}} \left(\frac{1}{\varepsilon_{sl}} - 1 \right) \right]^{-1}. \quad (11)$$

In steady state Q_r is also equal to

$$Q_r = h_{sl} A_{sl} (T_{sl} - T_{a,av}), \quad (12)$$

$$Q_c = h A_{su} (T_{su} - T_{a,av}) \quad (13)$$

$$Q = h_{cn} A_{su} (T_{su} - T_{a,av}), \quad (14)$$

$T_{a,av}$ is the average temperature of air along the annular flow, which can be given as $T_{a,av} = ((T_2 + T_3)/2)$, where T_2 and T_3 are inlet and outlet air temperature for annular air flow; h , convection heat transfer coefficient; h_{cn} , equivalent convection heat transfer coefficient from storage unit surface to air; h_r , equivalent radiation heat transfer coefficient based on $T_{su} - T_{sl}$ (annular flow); h_{sl} , convection heat transfer coefficient from the sleeve to the annulus air flow; $T_{a,av}$, average air temperature along the annulus flow in the storage unit; h_{cn} , and h_r can be given as:

$$h_{cn} = h + h_r \frac{T_{su} - T_{sl}}{T_{su} - T_{a,av}}$$

$$h_r = \sigma \varepsilon \frac{T_{su}^4 - T_{sl}^4}{T_{su} - T_{sl}}$$

Heat transfer coefficient for natural convection is given as (McAdams, 1954).

$$\frac{hL}{K_a} = Nu = C(Gr.Pr)^{n1}. \quad (15)$$

Here L is the characteristic length, which is the height of storage unit. Constants C and $n1$ depend upon $Gr.Pr$.

Average temperature within the storage unit are given by the following equations:

$$T_{su} = T_{a,av} + Q/(h_{cn} A_{su}) \quad (16)$$

$$T_{cs} = T_{a,av} + Q/(U A_{su}) \quad (17)$$

$$T_{cl} = T_{cs} + (q' R_1^2 / 4K_{vw}) \quad (18)$$

$$T_{sl} = T_{a,av} + Q_r/(h_{sl} A_{sl}) \quad (19)$$

Where U is the overall heat transfer coefficient based on the outer surface of the storage unit and q' is the heat generation rate.

The overall heat transfer coefficient from canister surface to the annulus air flow of the storage unit is given as:

$$U = \frac{1}{C_1 + C_2 + C_3 + C_4} \quad (20)$$

where C_1 , C_2 , C_3 and C_4 are thermal resistances, which can be given as:

$$C_1 = (h_{cn})^{-1}$$

(film resistance from storage unit surface to annular flow),

$$C_2 = \frac{R_4 \log_e(R_4/R_3)}{K_{su}}$$

(resistance across storage unit),

$$C_3 = \left[\varepsilon \sigma \frac{R_2 T_{cs}^4 - T_{su}^4}{R_4 T_{cs} - T_{su}} + \frac{K_a}{R_4 \log_e(R_3/R_2)} \right]^{-1}$$

(resistance across air gap)

$$C_4 = \frac{R_4 \log_e(R_2/R_1)}{K_s}$$

(resistance across waste canister),

$$\varepsilon = \left[\frac{1}{\varepsilon_{cs}} + \frac{A_{cs}}{A_{su}} \left(\frac{1}{\varepsilon_{su}} - 1 \right) \right]^{-1},$$

here ε is the equivalent emissivity considering the annular gap between the canister and the overpack.

2.1. 1-D heat transfer in overpack and sleeve

1-D heat transfer along the Z -direction has been considered for the storage unit and sleeve as shown in Fig. 5.

1-D steady state heat transfer equation for storage unit and sleeve can be given as (McAdams, 1954):

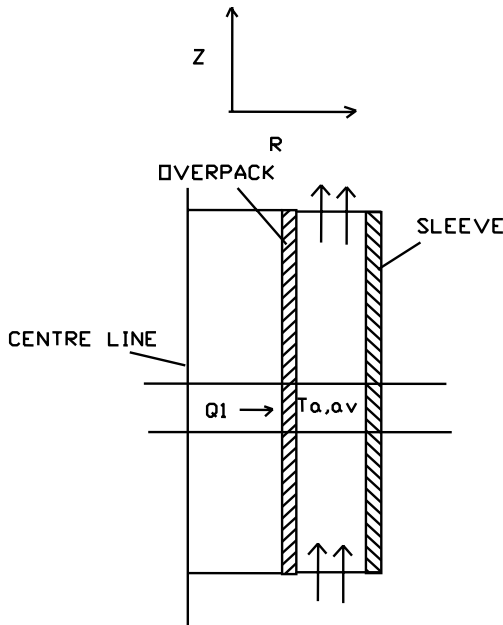


Fig. 5. Heat transfer in sleeve and the overpack.

$$\frac{\partial^2 T_{su}}{\partial Z^2} + \frac{1}{\alpha_{su} K_{su}} [Q_1 - h_{su} A_{su} (T_{su} - T_{a,av}) - \sigma \varepsilon A_{su} (T_{su}^4 - T_{sl}^4)] = 0 \quad (21)$$

$$\frac{\partial^2 T_{sl}}{\partial Z^2} + \frac{1}{\alpha_{sl} K_{sl}} [\sigma \varepsilon A_{su} (T_{su}^4 - T_{sl}^4) - h_{sl} A_{sl} (T_{sl} - T_{a,av})] = 0, \quad (22)$$

where K is the thermal conductivity for the respective case and α_{su} and α_{sl} are material volume of storage unit and sleeve, respectively. The above mentioned equations were discretized along the Z -direction and solved by the finite difference method. Adiabatic boundary conditions at the ends were assumed. Linear variation of the temperature of air within the annulus was assumed.

Q_1 can be given as (Fig. 5).

$$Q_1 = \pi R_1^2 q' \Delta Z. \quad (23)$$

2.2. Heat loss from the stack

The mode of heat transfer (Fig. 6) is assumed to be forced convection for the inner surface and natural convection and radiation for the outer surface.

In steady state, variation of inside air temperature with height can be given as:

$$\dot{m} C_p \frac{dT_{a,i}}{dZ} + h_{eq} A (T_{a,i} - T_{a,o}) = 0.$$

The solution of the above equation can be given as:

$$T_{a,i} = T_{a,o} - (T_{a,o} - T_o) e^{-h_{eq} A Z / \dot{m} C_p}, \quad (25)$$

where $T_{a,i}$, $T_{a,o}$ are the average values of temperature of air inside and outside the stack and T_o is the air temperature at the sack inlet. h_{eq} is the overall heat transfer coefficient from inner air to outer ambient based on outer surface of the stack and can be given as:

$$h_{eq} = \left[\frac{R_2}{R_1 h_{fr}} + \frac{R_2}{K_1} \log_e \frac{R_2}{R_1} + \frac{1}{h_{nat} + h_r} \right]^{-1}, \quad (26)$$

where h_{fr} , h_{nat} and h_r are heat transfer coefficient due to forced convection, natural convection and radiation equivalent. K_1 is the thermal conductivity of the stack material. R_1 and R_2 are the inner and outer radius of the stack.

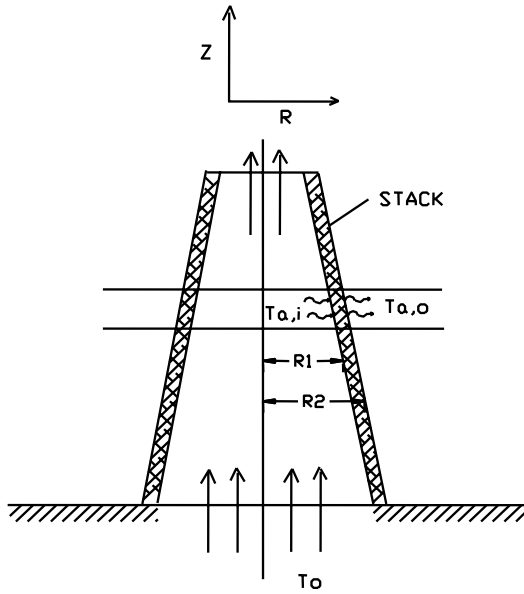


Fig. 6. Heat transfer from the stack.

Equivalent heat transfer coefficient for radiation from outer surface of stack can be given as:

$$h_r = \sigma \epsilon \frac{(T_s^4 - T_{a,o}^4)}{(T_s - T_{a,o})},$$

where T_s is the outer surface temperature of the stack.

Heat transfer coefficient for forced convection from inner surface can be given by the Dittus–Boelter Correlation (Kundsen et al., 1958).

$$h_{fr} = 0.023(Re)^{0.8}(Pr)^{0.4}K_a/D_e,$$

where D_e is the equivalent diameter of stack.

The heat transfer coefficient due to natural convection (h_{nat}) from outer surface of the stack to the outside ambient air and can be evaluated by using Eq. (15).

2.3. Heat loss from the vault

The heat loss from the vault is by natural convection from the inner wall and natural convection and radiation from the outer wall. The heat transfer from the inner surface and the outer surface of the roof are by natural convection and natural convection and radiation, respectively.

3. Experimental facility

For validation of the analytical results, an experimental facility was designed and fabricated (Babu Rajan, 2001). The set-up included 20 (5×4) number of storage units placed in a vault and a stack of height of 20 m and exit diameter of 0.30 m (Figs. 2 and 3). The salient details of the set-up are given in Table 2. Full height of storage unit (to be used in the waste storage facility) has been simulated with the sleeve. In this experimental facility heat is generated with the help of electrical heaters. Individual regulators have been used, for control of heat input for each storage unit. Thermocouples have been used at various places to measure the temperature such as on surface of storage unit, sleeve, upper and bottom plenum etc. The details regarding the position of thermocouples and other instrumentation are given in the Table 1 (Babu Rajan, 2001).

Temperatures was measured at the following locations:

1. overpack surface,
2. sleeve surface,
3. air at inlet duct,
4. air at the inlet and the outlet of the annulus flow,
5. air at upper plenum,
6. Outside ambient.

In the experimental facility, a number of thermocouples was installed such that the maximum temperature is faithfully recorded. The number of thermocouples, however, was restricted based on the number of openings. Care had also be exercised to keep the flow path resistances, hence the pressure drop, within reasonable limits. There was no direct measurement of flow rate or flow velocity.

3.1. Pre-test analysis

Pre-test theoretical predictions were made for the experiments carried out with all the storage units having the same heat input. The input for the theoretical analysis is shown in Table 2. The coefficients of pressure loss and heat loss were assumed in absence of measured data. These were generally based on bounding values obtained

Table 2
Input data

R_1 (m)	R_2 (m)	R_3 (m)	R_4 (m)	R_5 (m)	R_6 (m)	L (m)	
Storage unit data							
0.15	0.16	0.165	0.175	0.3	0.31	2.0	
Inlet	Outlet	Size (m ²)	Height	Diameter	Height	Length	Width
Duct length (m)							
1.0	2.0	0.21 × 0.21	Stack (m) 20	0.3	Vault dimension (m) 3.0 5.0 4.0		
Constant/properties							
Thermal conductivity (kW/m ^{−1} K ^{−1})							
Stack (mild steel)	Vault (galvanised mild steel)	Sleeve (steel)	Overpack (steel)	Air			
4.5E−02	6.5E−02	1.6E−02	1.6E−02	3.2E−05			
Stack	Vault	Sleeve	Overpack	Canister surface			
Emissivity							
0.5	0.1	0.1	0.1	0.1			

from the literature. The results are presented in Table 3 and discussed in the following section. The convective heat transfer coefficients are based on natural convection because the induced velocity in the annulus is of the order of 4 cm s^{-1} . At such a low velocity, heat transfer due to natural convection will dominate. The Gr/Re^2 is of order of 10^6 .

3.2. Experimental results

The experimental results (Babu Rajan, 2001) are shown in Table 3, which are compared with the theoretical analysis carried out (pre-test analysis). Temperatures are shown for various places. Since the mass flow rate was not measured directly, it was inferred from the heat balance equation as follows:

$$Q = \dot{m} C_p \Delta T, \quad (27)$$

where Q is the heat input, \dot{m} is the mass flow rate per overpack, C_p is the specific heat of the air and ΔT is the temperature rise of air between annulus outlet and inlet ($T_{\text{amb}} = 29.5 \text{ }^\circ\text{C}$) of an overpack.

In general, there is a good agreement for the

trends of the result. The predicted temperature at annulus outlet is approximately $10 \text{ }^\circ\text{C}$ higher than the measured value for power input of 0.16 kW per storage unit and this difference increases to $14.8 \text{ }^\circ\text{C}$ for power input of 0.49 kW per storage unit. The difference between the predicted and the measured value of temperature at stack inlet is $2.8\text{--}3.8 \text{ }^\circ\text{C}$.

The predicted maximum, minimum and the average values of surface temperature for overpack and sleeve and the maximum temperature observed in the experiment are also shown in the Table 3. The difference between predicted and measured value of the maximum temperatures are higher by $6.2\text{--}9.5 \text{ }^\circ\text{C}$ for overpack and $7.2\text{--}11.0 \text{ }^\circ\text{C}$ for sleeve. Table 3 further shows the theoretical and projected value of the mass flow rate. The projected value from the experimental analysis is obtained by the (Eq. (27)).

The predicted and experimental (projected in case of mass flow rate) values of mass flow rate, annulus outlet temperature, stack inlet temperature, overpack surface temperature and sleeve surface temperatures with respect to heat input are shown in Fig. 7A and B.

Table 3
Results from pre-test analysis and experimental observations

Sl. no.	Power per overpack (kW)	Mass flow rate (kg s ^{−1})	Temperature (°C)					Overpack	Sleeve
			Air						
			Annulus inlet	Annulus outlet	Upper plenum	Stack inlet	Stack outlet		
1	0.16	0.096	T_{amb}	62.6		49.8	40.8	71.2 (max) 48.3 (min) 62.7 (av)	58.3 (max) ^a 38.9 (min) ^a 51.1 (av) ^a
		0.138	38	52.5	50	46.0	65.0 (max)	51.0 (max) ^b	
		0.106	T_{amb}	69.1		54.3	43.7	80.9 (max) 53.5 (min) 70.6 (av)	64.5 (max) ^a 41.2 (min) ^a 55.5 (av) ^a
2	0.21	0.137	40	60.0	55	51.8		77.0 (max)	58.0 (max) ^b
		0.122	T_{amb}	83.1		64.1	49.8	102.6 (max) 65.8 (min) 88.4 (av)	78.4 (max) ^a 46.4 (min) ^a 65.5 (av) ^a
		0.162	42	70.0	66	61.6		98.0 (max)	70.1 (max) ^b
3	0.33	0.139	T_{amb}	99.8		75.8	57.3	129.5 (max) 81.7 (min) 110.9 (av)	96.0 (max) ^a 53.2 (min) ^a 78.3 (av) ^a
		0.176	43	85.0	80	73.0		120.0 (max)	85.0 (max) ^b

$T_{\text{amb}} = 29.5$ °C; stack height = 20.0 m; stack diameter = 0.305 m.

^a Theoretical.

^b Experimental.

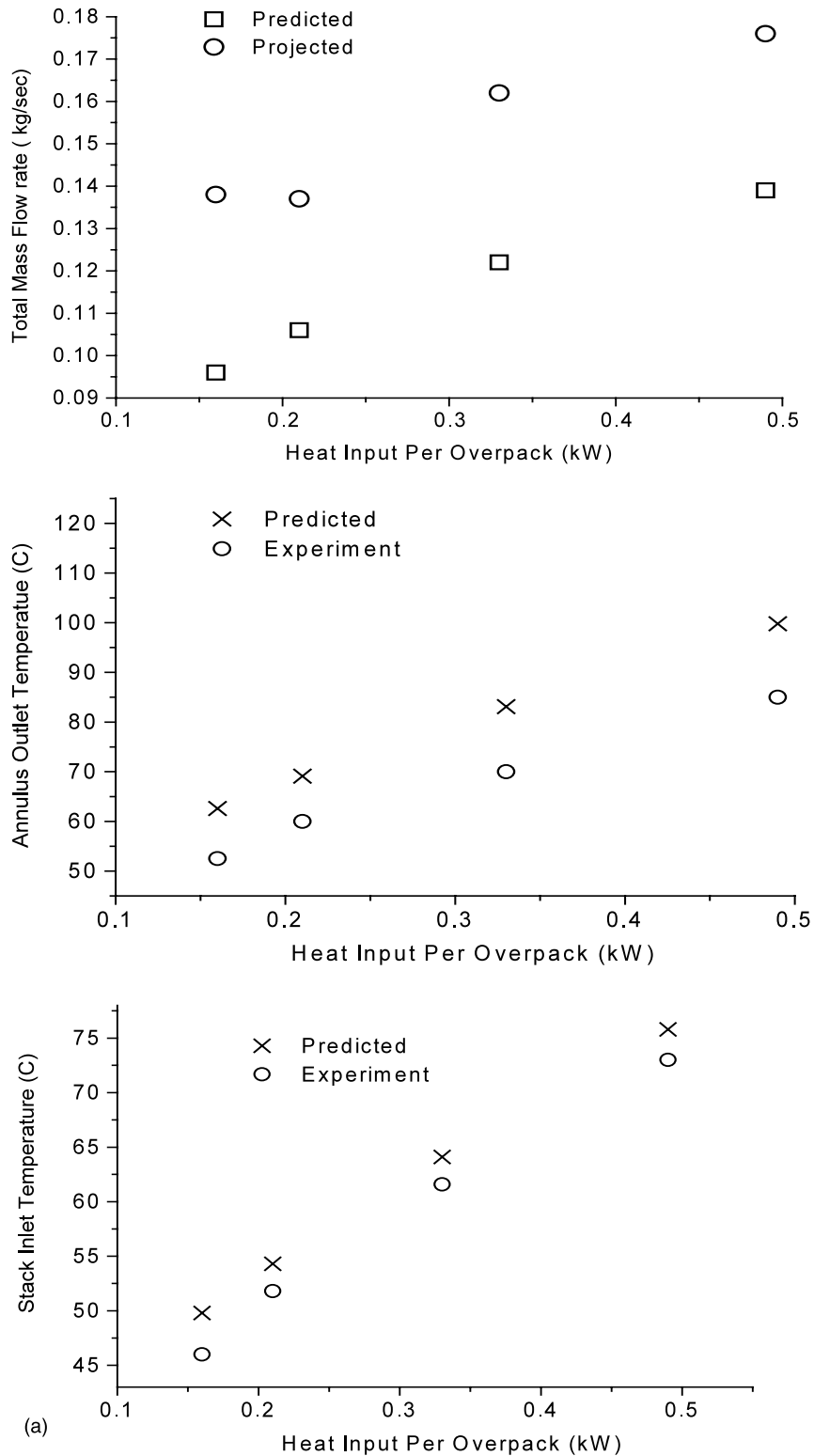


Fig. 7. (a) Results from pre-test analysis and experimental observations; (b) results from pre-test analysis and experimental observations.

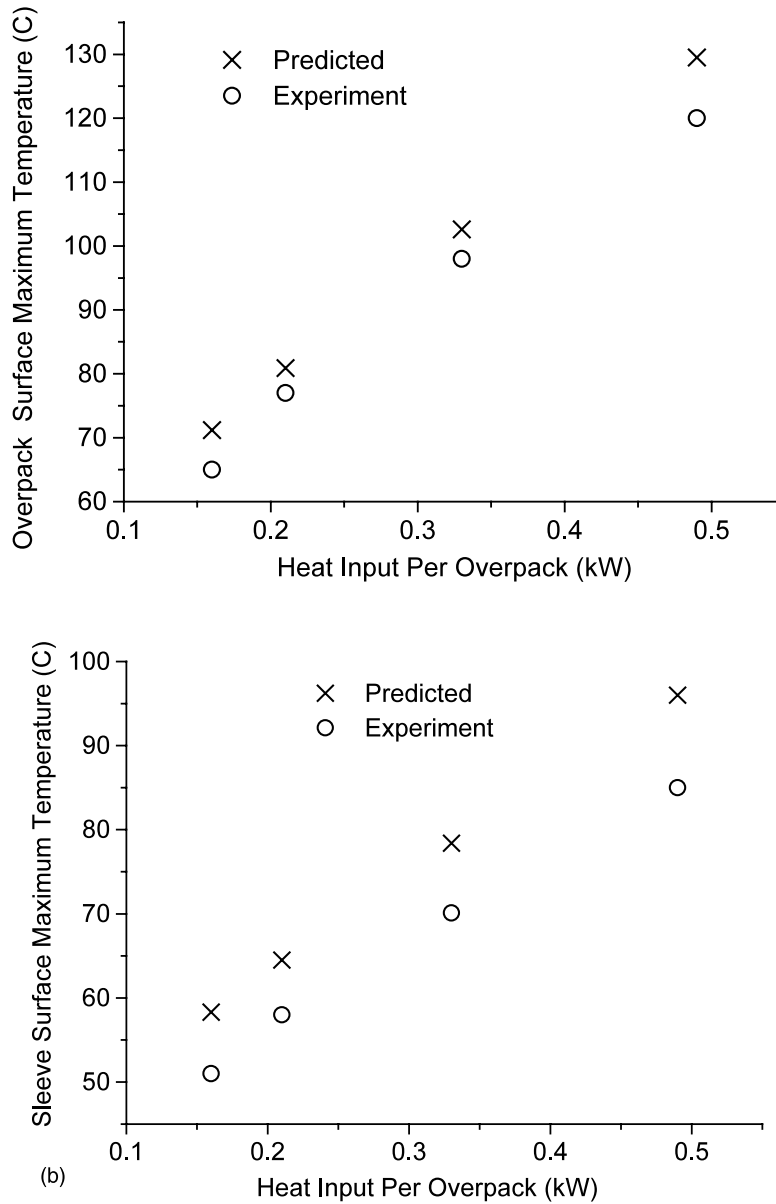


Fig. 7. (Continued)

3.3. Post-test analysis

It may be seen that the mass flow rate calculated by theoretical analysis is lower. This may be due to a higher assumed value of loss coefficient for various junctions.

The values of the loss coefficients for sudden contraction and expansion were chosen on the basis of values given in the literature and generally fixed at the maximum values in the range. However, without any experimental verification these numbers could not have been specified bet-

Table 4
Results from post-test analysis and experimental observations

Sl. no.	Power per overpack (kW)	Mass flow rate (kg s ⁻¹)	Temperature (°C)					Overpack	Sleeve
			Air						
			Annulus inlet	Annulus outlet	Upper plenum	Stack inlet	Stack outlet		
1	0.16	0.120	T_{amb}	55.9		48.5	40.8	65.6 (max)	53.0 (max) ^a
								47.3 (min)	37.5 (min) ^a
		0.138	38	52.5	50	46.0		59.2 (av)	47.5 (av) ^a
2	0.21	0.132	T_{amb}	61.2		52.5	43.5	65.0 (max)	51.0 (max) ^b
								74.2 (max)	58.1 (max) ^a
		0.137	40	60.0	55	51.8		52.3 (min)	39.5 (min) ^a
3	0.33	0.153	T_{amb}	72.4		61.3	49.4	66.5 (av)	51.2 (av) ^a
								77.0 (max)	58.0 (max) ^b
		0.162	42	70.0	66	61.6		93.7 (max)	69.6 (max) ^a
4	0.49	0.173	T_{amb}	85.7		71.8	56.5	64.2 (min)	44.0 (min) ^a
								82.9 (av)	59.6 (av) ^a
		0.176	43	85.0	80	73.0		98.0 (max)	70.1 (max) ^b
								117.9 (max)	84.2 (max) ^a
								79.7 (min)	50.1 (min) ^a
								103.7 (av)	70.5 (av) ^a
								120.0 (max)	85.0 (max) ^b

$T_{\text{amb}} = 29.5$ °C; stack height = 20.0 m; stack diameter = 0.305 m.

^a Theoretical.

^b Experimental.

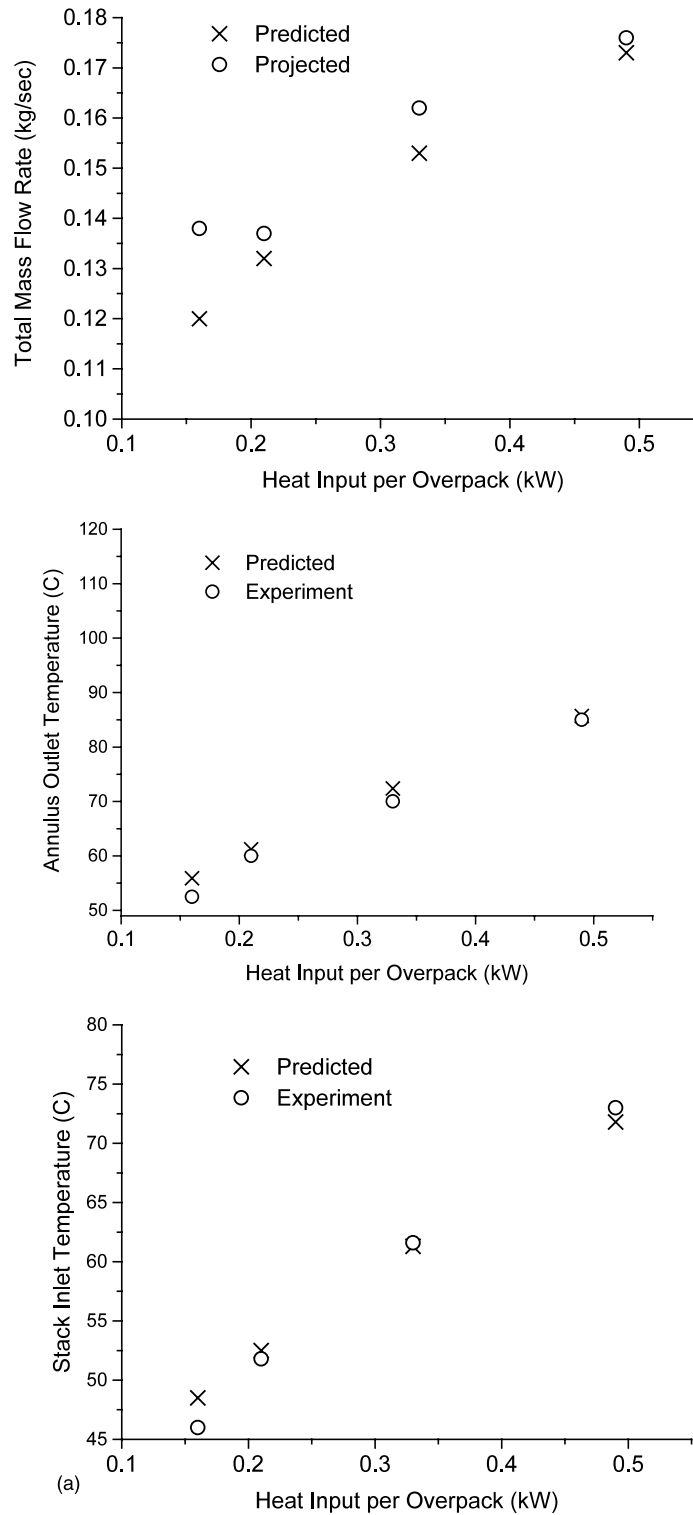


Fig. 8. (a) Results from post-test and experimental observations; (b) results from post-test and experimental observations.

Table 5
 Constants for axial flow $Nu = C(Gr.Pr)^{n1}$

$Gr.Pr$	C	$n1$
$< 10^4$	0.53	1/4
$10^4 - 10^9$	0.59	1/4
$10^9 - 10^{12}$	0.13	1/3

ter. The emissivity also depends upon the number factors such as surface finish, temperature, material, colour of the surface etc.

For post-test analysis the flow resistance and emissivity (for vault heat loss) are adjusted for a close match of the predicted and the measured values of flow rate for the case with power input of 0.49 kW per overpack (Sr. No. 4. of Table 3). Subsequently, results for all the cases were gener-

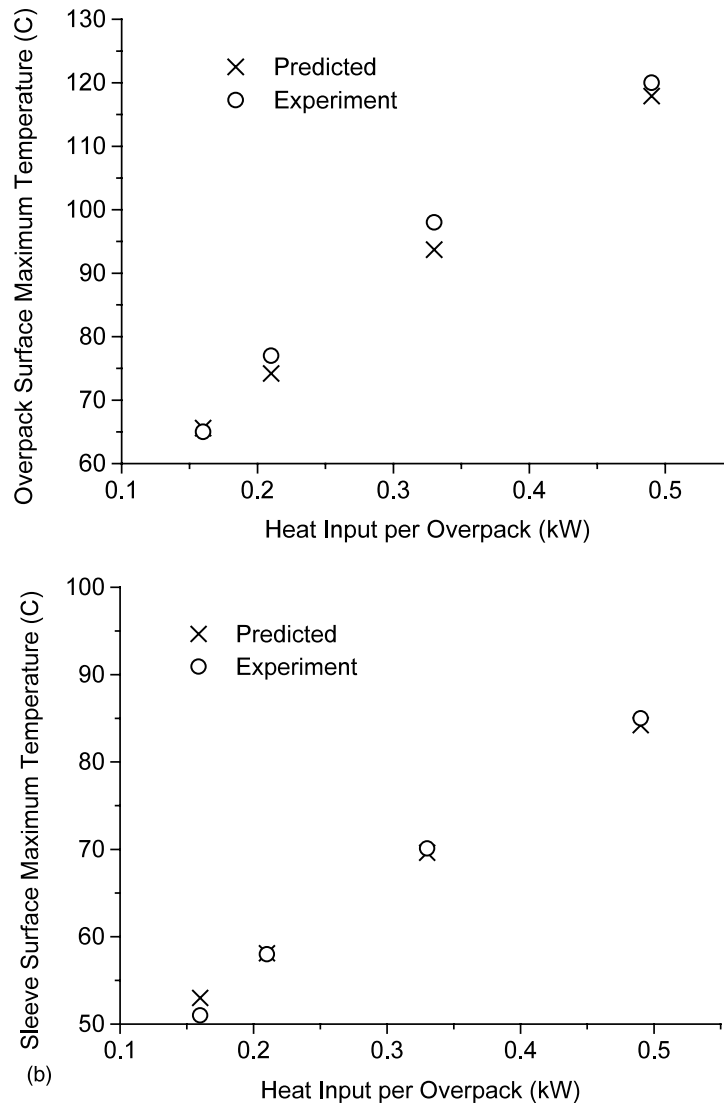


Fig. 8. (Continued)

Table 6
Sensitivity analyses

Emissivity	Maximum air temperature (°C)	Stack inlet air temperature (°C)	Stack outlet air temperature (°C)	Mass flow rate (kg s ⁻¹)
<i>Vault emissivity</i>				
0.5	99.85	75.85	57.3	0.1386
0.75 (25% higher)	100.4	74.83	56.7	0.1375
0.25 (25% lower)	99.12	77.2	59.3	0.14006
Coefficient of Blasius equation	Maximum air temperature (°C)	Stack inlet air temperature (°C)	Stack outlet air temperature (°C)	Mass flow rate (kg s ⁻¹)
<i>Coefficient of Blasius equation</i>				
0.079	99.85	75.85	57.3	0.1386
0.0869 (10% higher)	100.4	76.07	57.4	0.1375
0.0711 (10% lower)	99.31	75.62	57.27	0.1397
Loss coefficients (Cg)	Maximum air temperature (°C)	Stack inlet air temperature (°C)	Stack outlet air temperature (°C)	Total mass flow rate (kg s ⁻¹)
<i>Loss coefficients</i>				
<i>Exit of inlet duct</i>				
1.0	99.85	75.85	57.3	0.1386
0.75 (25% lower)	98.08	75.11	57.11	0.1422
<i>Entry of annulus</i>				
0.5	99.85	75.85	57.3	0.1386
0.375 (25% lower)	99.85	75.85	57.3	0.1386
<i>Exit of annulus</i>				
1.0	99.85	75.85	57.3	0.1386
0.75 (25% lower)	99.85	75.85	57.2	0.1386
<i>Entry of outlet duct</i>				
0.5	99.85	75.85	57.3	0.1386
0.375 (25% lower)	98.83	75.42	57.2	0.1407
<i>Exit of the outlet duct</i>				
1.0	99.85	75.85	57.3	0.1386
0.75 (25% lower)	97.80	75.0	57.1	0.1428

ated by using these parameters. Results for the post-test analysis is shown in Table 4.

The post-test analysis shows that the projected mass flow rate, annulus outlet temperature and stack inlet are now in much better agreement with experimental observations. The overpack and sleeve temperature are also shown in the Table 4.

The theoretical (post-test) and experimental (projected incase of mass flow rate) values of mass flow rate, annulus outlet temperature, stack inlet temperature, overpack surface temperature and

sleeve surface temperatures with respect to heat input are shown in Fig. 8 a and b.

4. Discussion

Pre-test analysis results are based on the bounding values of the loss coefficients obtained from literature such as entry loss coefficient of 0.5 and exit loss coefficient of 1.0. Exact value of loss coefficients depends upon a number of parameters

such as geometrical dimensions, surface roughness, velocity etc. The coefficients of pressure drop were assumed in absence of measured data. The coefficients for the heat transfer (Eq. (15)) are given in Table 5.

In the experiment, mass flow rate was not measured. It was inferred from the heat balance equation (Eq. (27)).

Sensitivity analyses for vault emissivity, coefficient of Blasius equation and the loss coefficients at different junctions have been carried out which show that the individual effect is not significant. These results are presented in Table 6.

5. Conclusion

Theoretical and experimental results have been compared, which are in good agreement. 1-D analysis appears to be adequate for the present configuration and condition of uniform heating in all the overpacks.

Acknowledgements

The authors thank S.D. Mishra, Head, WMPD, P.M. Gandhi, P.D. Ozarde and G. Rajani of the Waste Management Projects Division for many useful discussion and help at various stages of the work.

Appendix A. Nomenclature

A	area (m^2)
C_p	specific heat ($\text{kW kg}^{-1} \text{K}^{-1}$)
D_e	hydraulic diameter (m)
f	fanning friction factor
f_w	friction factor (Darcy–Weisbach equation)
g	acceleration due to gravity (m s^{-2})
Gr	Grashoff number
h	heat transfer coefficient ($\text{kW m}^{-2} \text{K}^{-1}$)
K	thermal conductivity ($\text{kW m}^{-1} \text{K}^{-1}$)
L	length (m)

Nu	Nusselt number
\dot{m}	mass flowrate (kg s^{-1})
P	pressure (N m^{-2})
Pr	Prandtl number
q'	heat generation rate (kW m^{-3})
R	radius (m)
Re	Reynolds number
T	Temperature (K)
ΔT	temperature difference (K)
ΔT_f	temperature rise for the annulus air flow (K)
U	overall heat transfer coefficient ($\text{kW m}^{-2} \text{K}^{-1}$)
V	velocity (m s^{-1})
Z	elevation difference (m)

Greek symbols

α	volume (m^3)
ε	emissivity
ρ	density (kg m^{-3})
$\bar{\rho}$	average density (kg m^{-3})
σ	Stefan Boltzman constant
∞	ambient

Subscripts

a	air
amb	ambient
a,i	inside air
a,o	outside air
av	average
cs	canister surface
cn	convection
eq	equivalent
fr	forced
nat	natural
sl	sleeve
sli	sleeve inner surface
slo	sleeve outer surface
su	storage unit
r	radiation
vw	vittrified waste

References

- Babu Rajan, P.K., 2001. Experimental Simulation of Intermediate Waste Storage Facility. M-tech. Thesis, Department of Mechanical Engineering, Indian Institute of Technology, Mumbai, India.

- Kundsén, James G., Katz, Donald L., 1958. Fluid Dynamics and Heat Transfer. McGraw-Hill, New York.
- McAdams, William H., 1954. Heat Transmission, 3rd ed. McGraw-Hill, New York.
- Ozarde, P.D., Rana, D.S., Sunder Rajen, N.S., May 1981. Natural Draught Air Cooling System for Interim Storage of Solidified High Level Radioactive Waste. Indo-Soviet Seminar on Radioactive Waste Management, Bombay, India.
- Verma, V., Ghosh A.K., Venkat Raj, V., Kakodkar, A., 1995a. Thermal Analysis of Solidwaste Storage Surveillance Facility, Paper No. 087, Proceedings of International Conference on Evaluation of Emerging Nuclear Fuel Cycle Systems, GLOBAL-95, France, September 1995.
- Verma, V., Ghosh, A.K., Venkat Raj, V., Rajani, G., Ozarde, P.D., Gandhi, P.M., Mishra, S.D., 1995b. Thermal design of air cooled vault for interim storage of vitrified high level waste. In: Srinivasa, S., Jaluria, Y. (Eds.), Proceedings of the 2nd ISHMT-ASME Heat and Mass Transfer Conference and 13th National Heat and Mass Transfer Conference, Karnataka Regional Engineering College, Surathkal, India, Heat and Mass Transfer 95. Tata McGraw-Hill, New Delhi, pp. 657–663.
- Wong, H.Y., 1977. Heat Transfer for Engineers, 1st ed. Longman, London.